

PILOT-LESS SYNCHRONIZATION RECEIVER FOR UWB-BASED WIRELESS APPLICATION

J.-H. Kim and Y.-H. You

uT Communication Research Center
Sejong University
98 Kunja-Dong, Kwangjin-Ku, Seoul 143-747, Korea

K.-I. Lee, K.-S. Jeong, and J.-H. Yi

YuJeong Systems Co. Ltd.
503 Dong-Il B/D, 826 Kuro-3Dong, Kuro-Ku, Seoul 152-879, Korea

Abstract—This paper suggests a pilot-less residual carrier frequency offset (CFO) estimator for ultra-wideband orthogonal frequency division multiplexing (UWB-OFDM) systems. The basic idea of our approach is based on the fact that two adjacent OFDM symbols carry the identical information in the UWB-OFDM system, thus removing the need of pilot symbols. To demonstrate the efficiency of the proposed pilot-less CFO estimator, analytical expression of the mean square error (MSE) is reported and comparisons are made with the conventional pilot-aided CFO estimator in terms of MSE and throughput.

1. INTRODUCTION

The ultra-wideband (UWB) technology is one of the most innovative and promising wireless means to enable cable-less transmission of high-speed data between close-by nodes [1–4]. The WiMedia Alliance has defined the inter-operability standards for UWB communication [5]. The work of the WiMedia Alliance has focused its efforts on providing increased capability to enable new high-rate wireless applications. There has been explosive adoption of UWB technology in the various wireless applications [6–10]. A particularly interesting potential WiMedia application is short-range wireless video transmission. Uniquely, the availability of broad spectrum in UWB communication

provides an unequalled advantage for high-performance and high-capacity wireless video networks [6]. Current wireless video solutions such as Wi-Fi do not have the bandwidth to accommodate high-definition (HD) or AVC/H.264 video streams, which require a minimum of 20 Mbps each. UWB can offer data-rates exceeding those that are required to convey high quality broadcast video and new features such as watching broadcast quality video over a broadcast-type wireless link will enable multimedia presentation in education, libraries, advertising, or have a wireless connection at home [11, 12].

High-rate UWB is an orthogonal frequency division multiplexing (OFDM) system designed to deliver data rates between 53.3 and 480 Mbps in pico-environments. In the WiMedia UWB system, frequency hopping (FH) and OFDM are used for high data-rate transmission, however this combination of FH and OFDM makes carrier frequency offset (CFO) a considerable problem [13, 14]. Even though most systems compensate the frequency offset with initial training sequences, there might still be a residual CFO. The uncompensated residual CFO can cause inter-carrier interference (ICI) and large signal constellation rotation. So it must be compensated, otherwise it would lead to degradation in system performance [15, 16]. A number of algorithms to remove the effect of CFO are presented in the literature using pilot subcarriers [13–20]. In the current WiMedia UWB system, only a few pilots are embedded in one OFDM symbol for frequency tracking. As a result, the major challenge in the UWB systems is to increase frequency estimation accuracy with the limited pilots.

In this paper, we present a fine synchronization receiver with algorithm for tracking of residual CFO for UWB-based video transmission applications. In order to design an improved synchronization receiver without the use of pilot symbols, some modifications on the current WiMedia UWB system are introduced. It is found that a slight modification leads to improved estimation performance in comparison with the traditional pilot-aided synchronization scheme. Since we save the pilots for synchronization, the throughput of the system is also increased. In order to show the usefulness of the proposed scheme, it is applied to H.264 based video communication system.

This paper is organized as follows: Section 2 describes the signal model for the UWB-OFDM system. In Sections 3, a pilot-less fine frequency estimation algorithm is suggested for UWB-OFDM system and its performance is reported in terms of mean square error (MSE). The simulation environment and detailed results are discussed in Section 4. Finally, conclusion are drawn in Section 5.

2. SYSTEM MODEL

Consider the UWB-OFDM system using N points of IFFT and N_{zp} zero-padded suffix. The transmitted baseband signal for the n -th sample of the l -th OFDM symbol $x_l(n)$ can be simply expressed as

$$x_l(n) = \frac{1}{\sqrt{N}} \sum_{k=-N/2}^{-N_n/2} X_l(k) e^{j2\pi nk/N} + \frac{1}{\sqrt{N}} \sum_{k=N_n/2}^{N/2-1} X_l(k) e^{j2\pi nk/N} \quad (1)$$

where $X_l(k)$ is the non-zero symbol transmitted on the k -th subcarrier and N_n is the number of null subcarriers.

At the receiver, we assume that the symbol timing error is perfectly compensated. Taking into account the small CFO, the received OFDM symbol after FFT demodulation becomes [19][21]

$$R_l(k) = G_l X_l(k) e^{j2\pi\Delta l(N+N_{zp})/N} \frac{\sin(\pi\Delta)}{N\sin(\pi\Delta/N)} H_l(k) + I_l(k) + W_l(k) \quad (2)$$

where G_l is the lognormal shadowing term, $H_l(k)$ is the channel's frequency response with zero-mean and variance σ_H^2 incorporating the time-invariant phase term, $W_l(k)$ is a zero-mean complex Gaussian noise term with variance σ_W^2 during the l -th symbol period, Δ is the CFO relative to the inter carrier spacing, and $I_l(k)$ is the ICI term. In Eq. (2), the ICI caused by small CFO can be omitted, since its power is very small compared with the additive noise power [21]. So, Eq. (2) can be simplified into

$$R_l(k) \approx C_l(k) X_l(k) e^{j2\pi\Delta l(N+N_{zp})/N} + W_l(k) \quad (3)$$

with denoting $C_l(k) = G_l H_l(k)$.

3. PILOT-LESS FINE FREQUENCY SYNCHRONIZATION RECEIVER

In order to estimate the frequency error without the use of pilot symbols, a simple way of implementing a fine frequency estimator is suggested in this section and its estimation performance is analytically derived.

3.1. Synchronization Algorithm

The current UWB-OFDM system provide time domain diversity by time-domain spreading (TDS) and frequency domain diversity by frequency domain spreading (FDS). Both FDS and TDS techniques shall be used when the data unit is encoded at a data rate of 53.3 or 80 Mb/s. When the data unit is encoded at data rate of 106.7, 160 or 200 Mb/s, only TDS technique is adopted. In this paper, we consider the UWB-OFDM system using only TDS for high-rate data transmission.

When the UWB-OFDM system is equipped with only TDS, in order to derive a pilot-less fine frequency estimator, the $(l + 1)$ -th OFDM symbol is modified into

$$X_{l+1}(k) = \text{Im}\{X_l(-k)\} - j\text{Re}\{X_l(-k)\} \quad (4)$$

where $\text{Re}\{x\}$ and $\text{Im}\{x\}$ denote the real and imaginary parts of x , respectively. It is noted from Eq. (4) that $x_{l+1}(k)$ can be effortlessly obtained from $x_l(k)$ without additional IFFT operation. At the receiver, the equalized signal is given by

$$\mathcal{R}_l(k) = R_l(k)\hat{C}_l^*(k) \quad (5)$$

where $\hat{C}_l(k)$ is the estimate of $C_l(k)$. Using the TDS property which is provided in the UWB-OFDM system, the fine frequency estimator is based on post-FFT temporal correlation by using $N_u = N - N_n - N_g$ non-zero data symbols, where N_g is the number of guard subcarriers.

By using the relation between two consecutive symbols $X_l(k)$ and $X_{l+1}(k)$ in Eq. (4), one can find that $X_l^*(k)X_{l+1}(-k) = (-j)|X_l(k)|^2$. When we consider the non-zero signal samples excluding the guard subcarriers in the UWB-OFDM system, a temporal correlation is devised to has the form

$$T_l(k) = j\mathcal{R}_l^*(k)\mathcal{R}_{l+1}(-k), \quad k \in \mathcal{S}_0 \cup \mathcal{S}_1 \quad (6)$$

where \mathcal{S}_0 denotes the set of subcarrier indices in the left half $k \in [-(N - N_g)/2 + 1, -N_n/2]$ and \mathcal{S}_1 denotes the set of indices in the right half $k \in [N_n/2, (N - N_g)/2 - 1]$. The temporal correlation is further derived by

$$T_l(k) = |G_l|^4 |H_l(k)H_{l+1}(-k)|^2 |X_l(k)|^2 e^{j2\pi\Delta(N+N_{zp})/N} + \hat{W}_l(k) + \alpha_1 I_l^1(k) + \alpha_2 I_l^2(k) + \alpha_1 \alpha_2 I_l^3(k) \quad (7)$$

where $\hat{W}_l(k)$ denotes the additive noise component, $\alpha_i = \hat{C}_{l+i-1}(k) - C_{l+i-1}(k)$, $\alpha_i I_l^i(k)$ is the noise term due to the imperfect channel

estimation (CE), and the product of two estimation error terms $\alpha_1\alpha_2 I_l^3(k)$ are negligible at the high SNR. In Eq. (7), the noise contribution $\hat{W}_l(k)$ reads

$$\begin{aligned} \hat{W}_l(k) = & j|G_l|^3|H_l(k)|^2 H_{l+1}^*(-k) X_l^*(k) W_{l+1}(-k) \\ & + j|G_l|^3|H_{l+1}(-k)|^2 H_l(k) X_{l+1}(-k) W_l^*(k) \\ & + j|G_l|^2 H_l(k) H_{l+1}^*(-k) W_l^*(k) W_{l+1}(-k), \end{aligned} \quad (8)$$

and CE-induced noise terms $\{I_l^i(k)\}$ are given by

$$\begin{aligned} I_l^1(k) = & |G_l|^3 H_l^*(k) |H_{l+1}(-k)|^2 |X_l(k)|^2 \\ & + j|G_l|^2 H_l^*(k) H_{l+1}^*(-k) X_l^*(k) W_{l+1}(-k) \\ & + j|G_l|^2 |H_{l+1}(-k)|^2 X_{l+1}(-k) W_l^*(k) \\ & + jG_l W_l^*(k) W_{l+1}(-k) H_{l+1}^*(-k), \end{aligned} \quad (9)$$

and

$$\begin{aligned} I_l^2(k) = & |G_l|^3 |H_l(k)|^2 H_{l+1}(-k) |X_l(k)|^2 \\ & + j|G_l|^2 H_l(k) H_{l+1}(-k) X_{l+1}(-k) W_l^*(k) \\ & + j|G_l|^2 |H_l(k)|^2 X_l^*(k) W_{l+1}(-k) + jG_l W_l(k) W_{l+1}^*(-k) H_l(k) \end{aligned} \quad (10)$$

where we omit the phase-rotated term due to Δ because the statistical property of $\hat{W}_l(k)$ and $I_l^i(k)$ is untouched.

Since $E\{\hat{W}_l(k)\} = 0$ and $E\{\alpha_i I_l^i(k)\} = 0$, it follows that

$$\sphericalangle \{E [T_l(k)]\} = 2\pi\Delta(N + N_{zp})/N \quad (11)$$

where \sphericalangle is the angle operation. For relatively large N_u , the proposed fine frequency estimator is based on the cumulative phases of $T_l(k)$ on negative and positive subcarriers given by

$$\phi_{l,i} = \sphericalangle \left\{ \sum_{k \in \mathcal{S}_i} T_l(k) \right\}, \quad i = 0, 1. \quad (12)$$

Similar to [18, 19], by using Eq. (12), the fine frequency estimator takes expression

$$\hat{\Delta} = \frac{N}{2\pi(N + N_{zp})} \frac{\phi_{l,0} + \phi_{l,1}}{2}. \quad (13)$$

3.2. Performance Analysis

To demonstrate accuracy of the proposed frequency estimator, we derive the error variance. In an analogy to [18][19], denoting $\rho = e^{j2\pi\Delta(N+N_{zp})/N}$ and making use of $\tan(a+b) \approx \tan(a) + \tan(b)$, we obtain

$$4\pi(\Delta - \hat{\Delta})(N + N_{zp})/N \approx \frac{\operatorname{Im} \left\{ \sum_{k \in \mathcal{S}_0} T_l(k)\rho \right\}}{\operatorname{Re} \left\{ \sum_{k \in \mathcal{S}_0} T_l(k)\rho \right\}} + \frac{\operatorname{Im} \left\{ \sum_{k \in \mathcal{S}_1} T_l(k)\rho \right\}}{\operatorname{Re} \left\{ \sum_{k \in \mathcal{S}_1} T_l(k)\rho \right\}} \quad (14)$$

with

$$\begin{aligned} \operatorname{Re} \left\{ \sum_{k \in \mathcal{S}_i} T_l(k)\rho \right\} &\approx \sum_{k \in \mathcal{S}_i} |G_l|^4 |X_l(k)|^2 |H_l(k)H_{l+1}(-k)|^2 \\ &= \frac{N_u}{2} E\{|G_l|^4\} E\{|X_l(k)|^2\} E\{|H_l(k)|^2\} E\{|H_{l+1}(-k)|^2\}. \end{aligned} \quad (15)$$

So, the error of the estimate has the form:

$$\hat{\Delta} - \Delta = \frac{1}{2\pi\lambda N_u E\{|G_l|^4\} E\{|X_l(k)|^2\} E\{|H_l(k)|^2\} E\{|H_{l+1}(-k)|^2\}} \operatorname{Im} \left\{ \sum_{k \in \mathcal{S}_0 \cup \mathcal{S}_1} \left[\hat{W}_l(k) + \alpha_1 I_l^1(k) + \alpha_2 I_l^2(k) \right] \rho \right\} \quad (16)$$

where $\lambda = (N + N_{zp})/N$. Since $E\{\hat{W}_l(k)\} = 0$ and $E\{\alpha_i I_l^i(k)\} = 0$, the variance of the noise contribution in Eq. (16) is given by

$$\begin{aligned} \sigma_N^2 &= \sum_{k \in \mathcal{S}_0 \cup \mathcal{S}_1} E \left\{ \left| \operatorname{Im} \left\{ \left[\hat{W}_l(k) + \alpha_1 I_l^1(k) + \alpha_2 I_l^2(k) \right] \rho \right\} \right|^2 \right\} \\ &= N_u E \left\{ \left| \operatorname{Im} \left\{ \left[\hat{W}_l(k) + \alpha_1 I_l^1(k) + \alpha_2 I_l^2(k) \right] \rho \right\} \right|^2 \right\}. \end{aligned} \quad (17)$$

The MSE of fine frequency estimator can be obtained after some straight forward calculations

$$E \left\{ |\hat{\Delta} - \Delta|^2 \right\} = \frac{1}{4\pi^2 \lambda^2 N_u} \left[\frac{2B_3}{\text{SNR} \cdot B_2^2} + \frac{1}{2\text{SNR}^2 \cdot B_2} + E\{|\alpha_i|^2\} \left(\frac{B_3}{B_2^2} + \frac{1}{2\text{SNR}^2 \cdot B_2} + \frac{1}{\text{SNR} \cdot B_2} + \frac{B_1}{2\text{SNR}^2 \cdot B_2^2} \right) \right] \quad (18)$$

where $\text{SNR} = \sigma_H^2 E_s / \sigma_W^2$, $E_s = E\{|X_l(k)|^2\}$, $B_1 = E\{|G_l|^2\}$, $B_2 = E\{|G_l|^4\}$, and $B_3 = E\{|G_l|^6\}$. When the least square (LS) channel estimation is used, $E\{|\alpha_i|^2\} = 1/\text{SNR}$.

4. SIMULATION RESULTS

In this section, extensive simulations are performed to verify the accuracy of the MSE analysis. In our simulations, 106.7Mbps UWB-OFDM system with $N = 128, N_n = 6, N_g = 10$, and $N_{zp} = 37$ is considered. Here, the UWB channel model (CM) that has been contributed in IEEE 802.15.SG3a is used in [22] and 10^4 realizations of each UWB channel model are used, one realization being applied along the frame duration. In this paper, we consider a pilot-aided estimator developed in [21] as reference, which only uses $N_p = 12$ pilot symbols put in subcarriers $k \in \{-55, -45, \dots, -5, 5, \dots, 45, 55\}$ [5].

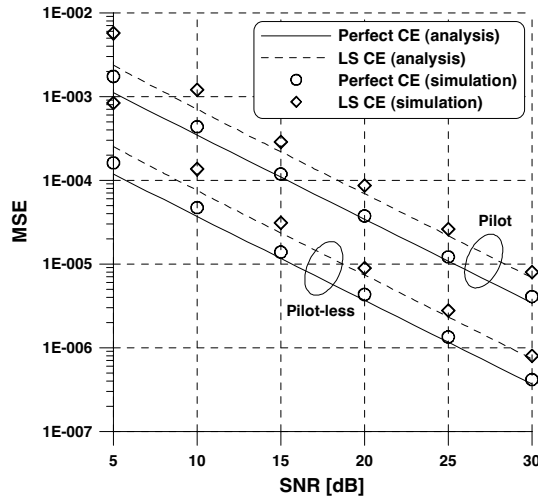


Figure 1. MSE performance of fine frequency estimators.

Figure 1 shows the MSE performance of fine frequency estimators in CM1. Here, we assume that the residual frequency error Δ is assumed to be 25% for ± 20 ppm frequency tolerance [5] and $N_n = 112$ non-zero data symbols are used for the pilot-less CFO estimation. When compared to the conventional method, the proposed method gives an improved estimation performance. The SNR difference between LS and perfect channel estimations is 3 dB. Therefore, one can expect that a sophisticated channel estimation scheme additionally improves the performance [23, 24]. More importantly, it is apparent that the theoretical results of fine frequency estimator according to Eq. (18) match with the simulation results very well with the increase of SNR.

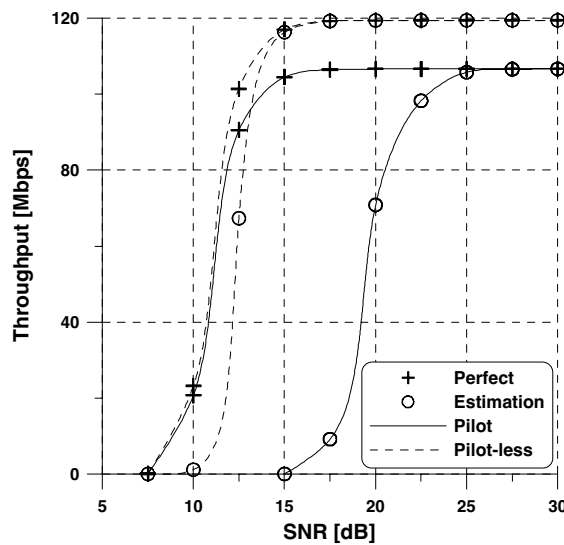


Figure 2. Throughput performance of fine frequency estimators.

In Fig. 2, the throughput performance of fine frequency estimators in CM1 is depicted. In this example, the results were based on a packet size of 1024 bytes and one-tap equalization is used. We can find that the pilot-less estimator gives very accurate performance, and it gives the almost same performance to perfect estimation case. When compared to the pilot-aided estimation method, the proposed UWB-OFDM receiver with pilot-less estimation provides approximately 12% throughput enhancement because we save the pilots for synchronization. However, the computational burden is increased by using all non-zero data information.

Figure 3 presents the average peak signal-to-noise ratio (PSNR)

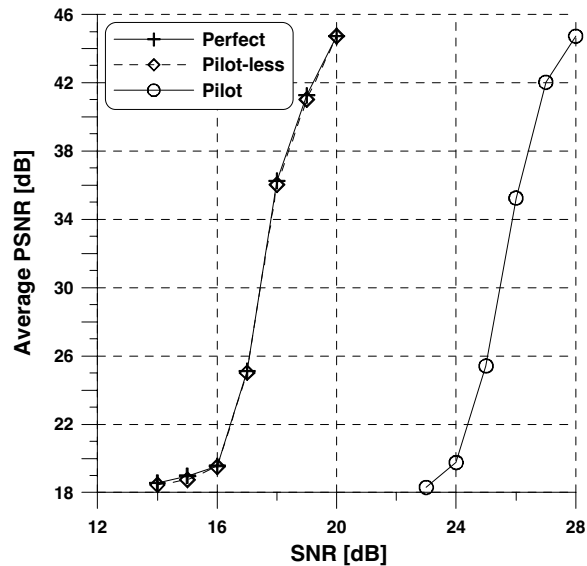


Figure 3. Average PSNR video quality of the UWB-OFDM synchronization receivers.

performance of the UWB-OFDM receiver with the pilot-less fine frequency estimator. In this example, LS channel estimation and one-tap equalization are used. The test video data is ballroom sequence whose resolution is 640×480 . In this simulation, the structure of GOP is “IPPPP...PIPP...”, where the size of GOP is 11, i.e., 10 P pictures are encoded between I pictures. With the help of 12% throughput enhancement in the pilot-less synchronization receiver, each I picture is transmitted repeatedly two times. The video codec used in this simulation is JM13.2 version. In order to check the usefulness of the proposed scheme, the average PSNR's of the encoded images are evaluated with respect to the original sequences at various SNRs, where the PSNRs are averaged values after simulations are repeatedly performed more than 100 times. As shown in Fig. 3, the PSNR's of the images resulted from the proposed pilotless scheme is much higher than those from the conventional system. It implies that the proposed algorithm increases the efficiency of the video communication system.

Figures 4–6 show the MSE and BER performances of fine frequency estimators when CM2~CM4 are used, respectively. The MSE and BER performances in CM2 are approximately parallel to these in CM1. When the system is encountered with high dispersive UWB channels CM3 and CM4, the error floor for all estimators can

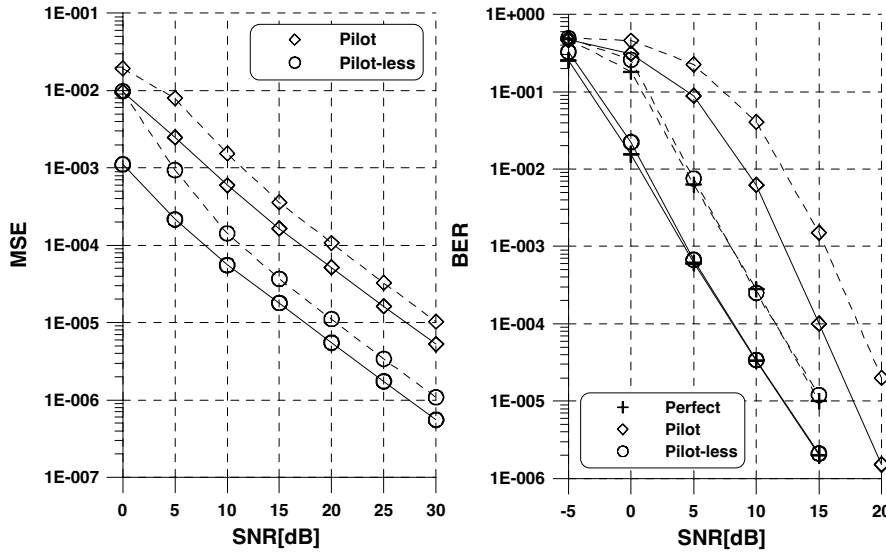


Figure 4. MSE and BER performances of fine frequency estimators in CM2: (1) solid lines - perfect CE (2) dashed lines - LS CE.

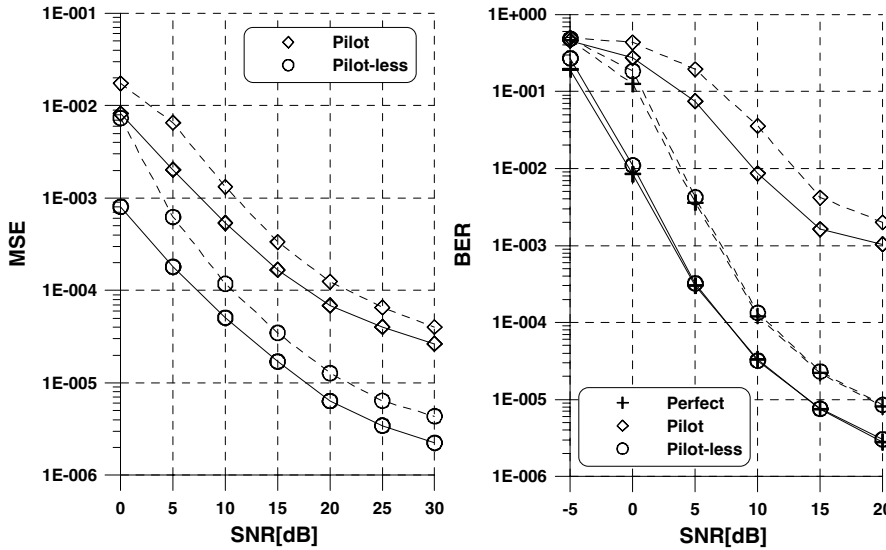


Figure 5. MSE and BER performances of fine frequency estimators in CM3: (1) solid lines - perfect CE (2) dashed lines - LS CE.

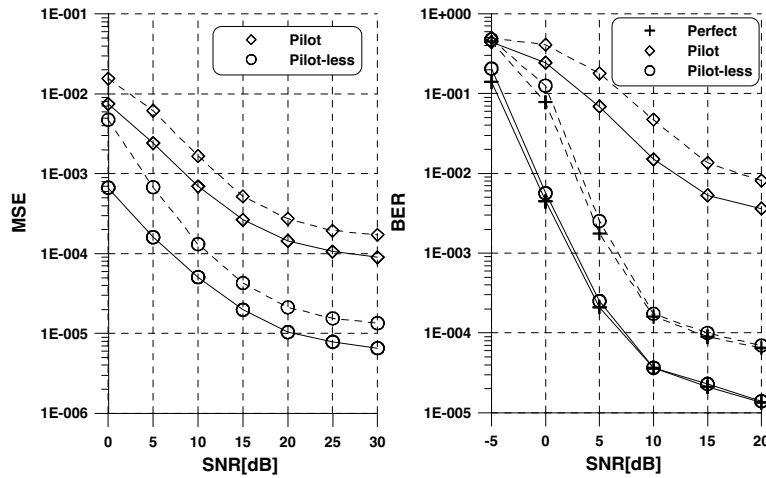


Figure 6. MSE and BER performances of fine frequency estimators in CM4: (1) solid lines - perfect CE (2) dashed lines - LS CE.

be observed because the delay spread of the channel is relatively longer than CM1 and CM2, which causes the inter-symbol interference. However, the performances of the proposed pilot-less estimator in CM3 and CM4 are also enhanced and come close to perfect estimation case, with the comparison with these of the pilot-aided conventional estimator.

5. CONCLUSION

In OFDM-based wireless UWB systems, a residual frequency offset introduces time and subcarrier varying phase rotations, which seriously degrade the performance of the systems. In this paper, we addressed the problem of estimating the residual frequency error for UWB-based wireless transmission systems without the aid of pilot information. Analytical expression of the MSE of the fine frequency synchronization scheme was derived and simulation results verified the accuracy of our MSE analysis.

ACKNOWLEDGMENT

The authors wish to acknowledge the assistance and support of the Center for Advanced Transceiver Systems and the Ministry of Commerce, Industry and Energy of Korea, and this research is supported by Seoul R&BD Program.

REFERENCES

1. Fan, Z. G., L. X. Ran, and J. A. Kong, "Source pulse optimizations for UWB radio systems," *Journal of Electromagnetic Waves and Applications*, Vol. 20, No. 11, 1535–1550, 2006.
2. Soliman, M. S., T. Morimoto, and Z. I. Kawasaki, "Three-dimensional localization system for impulsive noise sources using ultra-wideband digital interferometer technique," *Journal of Electromagnetic Waves and Applications*, Vol. 20, No. 2, 515–530, 2006.
3. Chen, C.-H., C.-H. Liu, C.-C. Chiu, and T.-M. Hu, "Ultrawide band channel calculation by SBR/IMAG techniques for indoor communication," *Journal of Electromagnetic Waves and Applications*, Vol. 20, No. 1, 41–51, 2006.
4. Liu, Y. J., Y. R. Zhang, and W. Cao, "A novel approach to the refraction propagation characteristics of UWB signal waveforms," *Journal of Electromagnetic Waves and Applications*, Vol. 21, No. 14, 1939–1950, 2007.
5. ECMA International, Standard ECMA-368, "High rate ultra wideband PHY and MAC standard," December 2007.
6. WiMedia Alliance, "Presentation to DLNA," January 2007.
7. Xiao, S., J. Chen, X.-F. Liu, and B.-Z. Wang, "Spatial focusing characteristics of time reversal UWB pulse transmission with different antenna arrays," *Progress In Electromagnetics Research B*, Vol. 2, 223–232, 2008.
8. El-Fishawy, N., M. Shokair, and W. Saad, "Proposed MAC protocol versus IEEE802.15.3a for multimedia transmission over UWB networks," *Progress In Electromagnetics Research B*, Vol. 2, 189–206, 2008.
9. Khani, H. and P. Azmi, "Performance analysis of a high data rate UWB-DTR system in dense multipath channels," *Progress In Electromagnetics Research B*, Vol. 5, 119–131, 2008.
10. Yin, X.-C., C. Ruan, C.-Y. Ding, and J.-H. Chu, "A planar U type monopole antenna for UWB applications," *Progress In Electromagnetics Research Letters*, Vol. 2, 1–10, 2008.
11. Cui, W., P. Ranta, T. Brown, and C. Reed, "Wireless video streaming over UWB," *Proc. of ICUWB 2007*, 933–936, September 2007.
12. Kim, J., S. Lee, Y. Jeon, and S. Choi, "Residential HDTV distribution system using UWB and IEEE 1394," *IEEE Trans. Consumer Electronics*, Vol. 52, No. 1, 116–122, February 2006.

13. Yak, C., Z. Lei, S. Chattong, and T. Tjhung, "Timing synchronization and frequency offset estimation for Ultra-Wideband (UWB) multi-band OFDM systems," *Proc. of PIMRC 2005*, 471–475, September 2005.
14. Yinghui, L., T. Jacobs, and H. Minn, "Frequency offset estimation for MB-OFDM-based UWB systems," *Proc. of ICC 2006*, 4729–4734, June 2006.
15. Wang, X., T. T. Tjhung, Y. Wu, and B. Caron, "SER performance evaluation and optimization of OFDM system with residual frequency and timing offsets from imperfect synchronization," *IEEE Trans. Broadcasting*, Vol. 49, No. 2, 170–177, June 2003.
16. Ai, B., Z.-X. Yang, C.-Y. Pan, J.-H. Ge, Y. Wang, and Z. Lu, "On the synchronization techniques for wireless OFDM systems," *IEEE Trans. Broadcasting*, Vol. 52, No. 2, 236–244, June 2006.
17. Shim, E. S. and Y. H. You, "Parameter estimation and error reduction in multicarrier systems by time-domain spreading," *Progress In Electromagnetics Research B*, Vol. 7, 1–12, 2008.
18. Speth, M., S. A. Fechtel, G. Fock, and H. Meyr, "Optimum receiver design for OFDM based broadband transmission — Part II," *IEEE Trans. Commun.*, Vol. 49, 571–578, April 2001.
19. Shi, K., E. Serpedin, and P. Ciblat, "Decision-directed fine synchronization for OFDM systems," *IEEE Trans. Commun.*, Vol. 53, 408–412, March 2005.
20. Chih-Peng, L., C. Po-Lin, and L. Tsui-Tsai, "Residual carrier frequency offset tracking for OFDM-based systems," *Proc. of APCCAS 2004*, 989–992, December 2004.
21. Speth, M., S. A. Fechtel, G. Fock, and H. Meyr, "Optimum receiver design for wireless broad-band systems using OFDM — Part I," *IEEE Trans. Commun.*, Vol. 47, 1668–1677, November 1999.
22. Foerster, J., *Channel Modeling Sub-committee Report*, IEEE, 802.15-02/490r1-SG3a, February 2003.
23. Baek, M. S., M. J. Kim, Y. H. You, and H. K. Song, "Semi-blind channel estimation and PAR reduction for MIMO-OFDM system with multiple antennas," *IEEE Trans. on Broadcasting*, Vol. 50, No. 4, 414–424, December 2004.
24. Koo, B. W., M. S. Baek, and H. K. Song, "Multiple antenna transmission technique for UWB system," *Progress In Electromagnetics Research Letters*, Vol. 2, 177–185, 2008.